Int. j. adv. multidisc. res. stud. 2023; 3(1):229-233

Received: 19-11-2022
Accepted: 29-12-2022

International Journal of Advanced Multidisciplinary Research and Studies

ISSN: 2583-049X

A DFT study of the effects of gas molecular adsorption on the electronic properties of monolayer B_9C_9

[1] Tamadhur Alaa Hussein, [2] Abbas H Abo Nasria
[1, 2] Department of Physics, Faculty of Science, University of Kufa, Najaf, Iraq

Corresponding Author: **Tamadhur Alaa Hussein**

Abstract
To investigate the sensitive properties of tiny poisonous gas molecules NO, CO, SO and HCN on monolayer a boron carbon, the B_3LYP functional and 6-311G (d,p) basis -set computations were used. These are the gases have a significant environmental impact. Using charge transfer, adsorbent energy, adsorbent distance, and characteristics, the optimal adsorption point was determined among three adsorption sites. These gas molecules HCN, NO, CO, and SO are chemically adsorbed on a boron carbon monolayer, according to the adsorption electron localization- function and energy results. the results also show that there is a significant amount of electron transport in between B_9C_9 monolayer and CO gas after adsorption. This suggests that boron carbon monolayers are more susceptible to CO, NO, SO, and HCN adsorption than pristine and doped graphene. Besides that, the energy band gap and work function of a boron carbon monolayer are modified to varying degrees through small gas molecule adsorption. Our study would provide theories direction for useful applications.

Keywords: B_9C_9 Monolayer, Gas Adsorption, DFT, H_{OMO}, L_{UMO}

1. Introduction

In areas where air pollution levels exceed WHO guidelines, seven out of ten people live, Toxic gases such as HCN, NO, CO, and SO observed in very many industrial and chemical plants, which would include processing of natural gas and utilization, are a result of air pollution, Pollution causes ozone layer depletion, which is exacerbated by wastewater treatment and semiconductor manufacturing. Some toxic gases are invisible, cannot be smelled, or have no immediate effect. As a result, detecting them solely through human sense is impossible without the use of instruments or devices [1, 2]. As a matter of fact, gas sensors became necessary for detecting toxic gases and monitoring air pollution. To deal with these issues, researchers should actively have sought components that consume little energy, quickly respond, and have a high gas responsivity [3]. As a side effect, researchers noticed that two-dimensional monolayers have a large area of surface and are a new sensor type [4, 5]. The characteristics of monolayer graphene are impressive [6, 7], in addition to experimental and theoretical investigation into the advancement of amazingly sensing devices**.**

2. Details of Modeling and Computation

To complete the DFT computations in this study, the Gaussian 09 package was used [8, 9]. This software package employs both traditional as well as advanced quantum physics fundamentals, also there are various kinds of them. A fully functioning base set B3LYP / 6-311G (d, p) is employed to undertake full geometric optimization techniques of the absorption influence of mono B_9C_9 molecules on HCN, CO, NO, and SO gas [10]. The B3LYP / 6-311G basic functionality is one of the theorist subjects used for nanostructure systems [11, 12]. The Fermi energy and chemical potential of the compounds was calculated, as illustrated below:

$$\text{Fermi energy} = [E\text{-}_{Homo} + E\text{-}_{Lumo}]/2 \qquad (1)$$

Where:
$E\text{-}_{Homo}$: the energy of the highest-occupancy molecular- orbital.
$E\text{-}_{Lumo}$: the energy of the lower- unoccupied molecular- orbital. [13]

Furthermore, for example, the energy band gap in the state's energy state is identified as shown in:

energy band gap = $E\text{-}_{Luom} - E\text{-}_{Homo}$ (2)

The adsorbent energy E_{ads} was calculated using the remarkably similar formula:

$E_{ads} = E_{complex} - E_{molcules} + E_{gas}$ (3)

Where:

$E_{complex}$: The real energy of the molecule as a consequence of adsorption process. [14]

$E_{molcules}$: Without absorption, the total energy of the researched molecule. [15]

E_{gas}: A gas molecule's total amount of energy [16].

3. Results and discussions

3.1 Models are available of adsorption

As shown in Fig. 1, the B_9C_9 monolayer is composed of a single layer. The B_9C_9 monolayer contains two types of adsorption sites. The initial distance between the B_9C_9 substrate and the gas molecules is set to 2.5. Furthermore, the original orientation of the gas molecule is perpendicular to the substrate. Because gas molecules absorb in a variety of configurations, several insertion geometries must be considered. To that end, one gas molecule (CO, SO, NO, and HCN) at a distance of 2.5 over B atom and bridge. In contrast, one of the triatomic original orientations (HCN) is considered. The carbon atom in the HCN molecular is on top of the B-C in the parallel direction, in the second direction, while the C atoms of HCN point in the same directions towards the bridge in the B_9C_9 layer. The entire system can then be completely relaxed. The molecules' absorption energies will be used to determine how they interact with the B_9C_9 layer. According to the equation. The lower the E_{ad} value, the larger the adsorbent of gas molecules onto B_9C_9. For further research, the most energy-efficient adsorption designs are chosen.

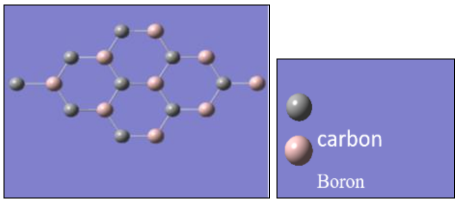

Fig 1: shows a monolayer's B_9C_9 geometric systems

According to Table 1, characteristics of the studied molecules such as Homo, Lumo, E_g, E_F, and E_T were calculated after working to improve the shape, electronic, and adsorption energy.

Table 1: B_9C_9 monolayer structural and electronic properties

Model	Site	LOMO	HOMO	E_g eV	E_F e.v
CO	Bridge	-0.1480	-0.1959	1.33868	-4.657317
	C	-0.12707	-0.19562	1.52343	-4.41276
SO	Bridge	-0.13685	-0.19506	1.34907	-4.63552
	C	-0.13744	-0.19724	1.62724	-4.55354
NO	Bridge	-0.16329	-0.17666	0.63593	-4.48919
	C	-0.14015	-0.18943	2.25731	-4.4481
HCN	Bridge	-0.13281	-0.16797	1.52098	-4.08231
	C	-0.12727	-0.19904	2.32507	-4.04149

The adsorption energies of various gas molecules used in this study on B_9C_9 are described in Table 1. Because we are only interested in the effect of adsorption process on the electronic configuration of the B9C9 monolayer, we ignore the varying effects of gas adsorption on the electronic configuration of the B9C9 single layer. on the other hand, a orientations of adsorption gas molecules. Electronic properties is based on descriptive of direction and adsorbent. t's advantageous to compare these molecules' adsorption energies in graphene even though they've been demonstrated to have superlative chemical sensing properties. The E_{ad} coefficients for CO on graphene-based B3LYP functional are estimated to be 0.8-1.4 eV. These results are lower than those obtained when adsorbed on B_9C_9, as illustrated in Table 1.

Table 2: Transfer charges Q, adsorption height D, and adsorption energies E_{ad} for various adsorption combinations

Gas	Location	(D) ˚A	(r)˚A	(E_{ad}) eV	(Q) |e|
CO	Bridge	2.15669	1.54	-0.3894	-0.01
	C	2.1558	1.54	-0.2509	-0.02
SO	Bridge	1.73492	1.85	-1.719	+0.10
	C	1.72769	1.85	-1.723	+0.12
NO	Bridge	1.37221	1.51	-2.247	-0.6
	C	1.32613	1.51	-2.303	-0.5
HCN	Bridge	2.06336	1.54	-0.114	-0.02
	C	2.06114	1.54	-0.264	-0.03

3.1.1 Adsorption of CO gas on a B_9C_9 monolayer

The adsorption of CO gas molecules on the B9C9 single layer is explored. Fig 2 shows the CO-B9C9 building's greatest stable adsorption structure. With adsorption energies of -2.8509˚A and -6.9894˚A, the CO gas is perpendicular to the B9C9 plane at two points the C atom and the B-C bridge. The mean atom-atom distance (C-C bond length) between CO and B9C9 is 2.1558˚A, which is larger than the C-C dimer bond length (1.54˚A), and the lowest atom-atom distance among CO and the bridge B-C is 2.15669˚A, which is larger than the B-C dimer bond length (1.54˚A). These findings suggest that CO physically adsorbs on the B_9C_9 layer.

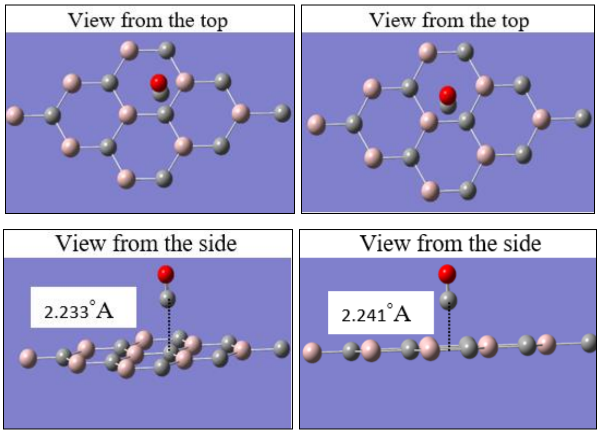

a) (b)

Fig 2: A most stable structures of (a) C-atoms (b) the bridge, B_9C_9 monolayer molecule adsorbed CO gas on the B_9C_9 top site is shown in top and the bottom views

3.1.2 SO gas Adsorption on B_9C_9 monolayer

The adsorption of SO gas molecules on a B_9C_9 monolayer is investigated. Fig 3 depicts the SO/ B_9C_9 complex's most stable adsorption structure. At two points, the SO molecule is perpendicular to the B9C9 plane: the atom and the B-C bridge. The adsorption energies for B9C9 are -1.719 and -1.723, respectively. The mean atom-atom distance (S-C bond length) between SO and B_9C_9 is 1.72769, which is less than the sum of S-C covalent atomic radii (1.85). These findings indicate that SO is chemically adsorbent.

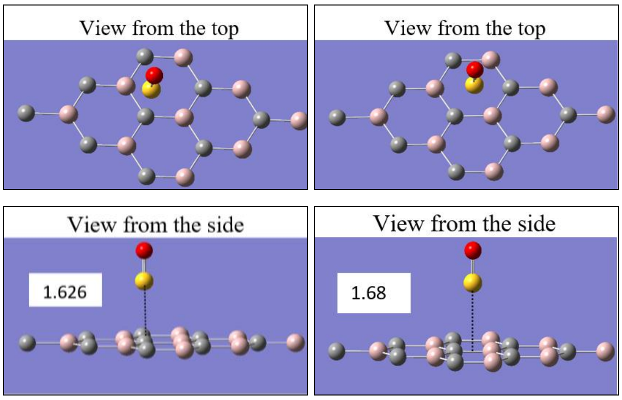

a) b)

Fig 3: The most stable structures of (a) S atoms, (b) bridge, and adsorption SO on the top site of B9C9 are shown in top and side views

3.1.3 Adsorption of NO gas on the B_9C_9 monolayer

(NO) gas moves in an oblique direction to the B9C9 level when revealed to the B9C9 layer, as shown in Fig. 3. The C atom is represented by the N atom of the NO gas in the B9C9. The O-N-C angle is 120.27 degrees, and the atom and B-C bridge adsorption energies for B9C9 are -2.247 and -2.303, respectively. The mean atom-atom length (N-C bond length) between NO and B9C9 is 1.32613, which is shorter than the N-C dimer bond length (1.51), and the lowest atom-atom distance (N-C bond length) between NO and the bridge B-C is 1.37221, which is shorter than the N-C dimer bond length (1.51). These findings indicate that gas (NO) is adsorbing chemically on the B9C9 layer.

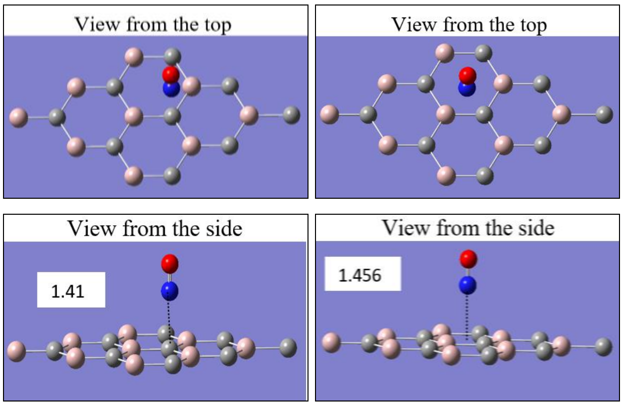

Fig 4: Bottom and side views of the more stable structures of (a) S atoms, (b) bridge, and (c) adsorbed gas (NO) on the top site of B_9C_9

3.1.4 HCN gas adsorption on the B_9C_9 monolayer

Gas (HCN) adsorption on B_9C_9 monolayers is much more difficult than that of the other molecules discussed previously. A gas runs parallel to and above the B_9C_9 monolayer, with the carbon atom in the gas (HCN) molecule located it above C in the B_9C_9. A adsorbent energies of gas (HCN) and B_9C_9 are -0.114 and -0.264, respectively, and the mean atom-atom length (C-C) among them is 2.06, which is larger than the C-C dimer bond (1.54) and the atom-bridge distance between gas (HCN) and monolayer B9C9 is (1.54) The results show that gas HCN is physically adsorption on the B9C9 single layer.

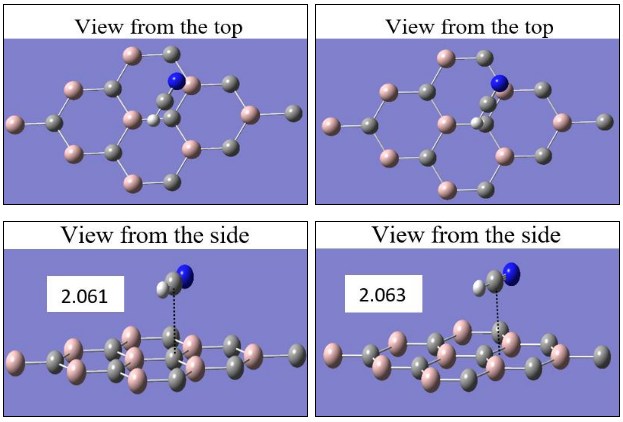

a) (b)

Fig 5: The most stable structures of (a) a C-atom, (b) a bridge, with HCN gas adsorbed on the top and bottom site of the B_9C_9

3.1.5 The B_9C_9 monolayer's electronic structure

Because the Homo and Lumo orbits are close to the Fermi plane, we can learn about electron states at the Fermi surface as well as transported electrons. Fig 6 depicts the orbital distributions of E_{homo} and E_{lumo}. Even though we found, the electron cloud distribution in these two orbits is focused at the edge of the B_9C_9 monolayer, where the electrons are focused. Fig 6 depicts the HOMO and LUMO energies of the B_9C_9 monolayer after gas absorption. SO and NO had no effect on the Ef of the pristine and B_9C_9 monolayer systems due to the short absorption distance, high charge transfer, and low absorption energy.

Gas	Site	E_{homo}		E_{lumo}
CO	Bridge	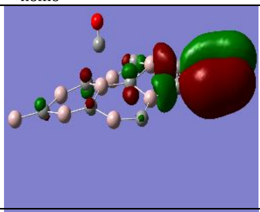	Eg (eV) 1.43967	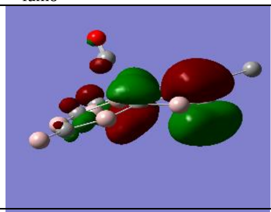
	C	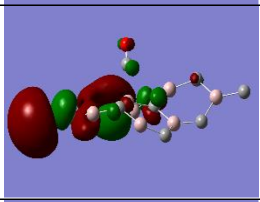	Eg(Ev) 1.532	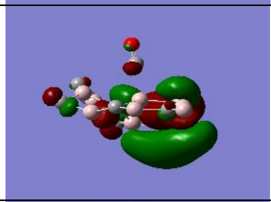
SO	Bridge	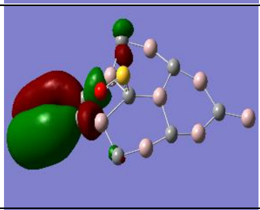	Eg (Ev) 1.443	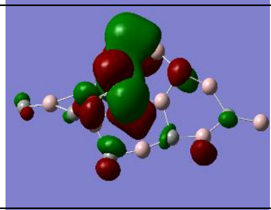
	C	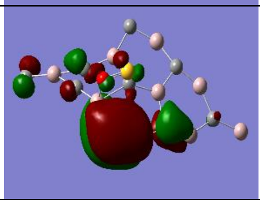	Eg (eV) 1.566	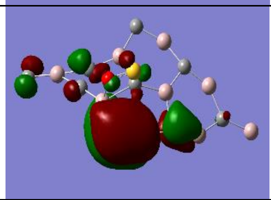
NO	Bridge	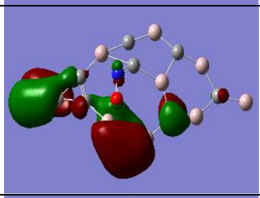	Eg (eV) 0.593	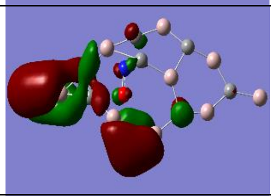
	C	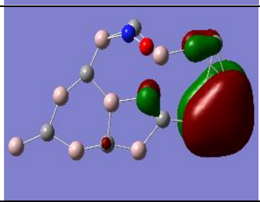	Eg (eV) 2.257	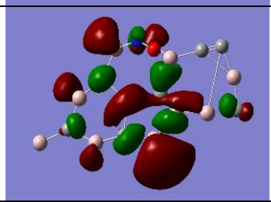
HCN	Bridge	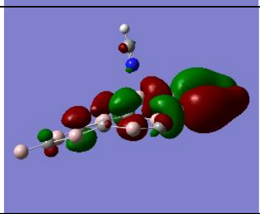	Eg (eV) 1.601	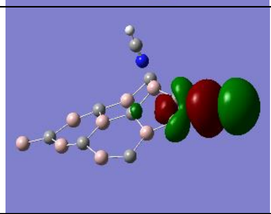
	C	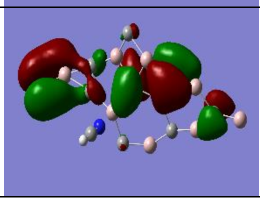	Eg (eV) 2.12507	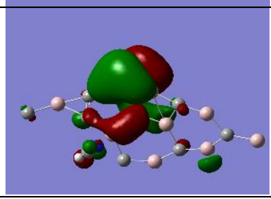

Fig 6: A B9C9 monolayer's electronic configuration

4. Conclusion

According to the DFT theoretical results, when B_9C_9 monolayers are revealed to normal and polluted gas molecules, they display a variety of behavior patterns. CO, SO, NO, and HCN molecules are attracted to the B_9C_9 monolayer more strongly. With broad Ead charge transfer, the chemical adsorption character of SO and NO adsorptions could be directly determined. In addition to HCN and CO physical adsorption. As a result, the B_9C_9 layers is a likely contender for gas sensing such as SO, CO, NO, and HCN.

5. References

1. John A, Herbert M, Muhammad S, Bilal Ahmad Farooqi, Umar Farooq, Muhammad Salman, Khurshid Ayub. Theoretical Approach to Evaluate the Gas-Sensing Performance of Graphene Nanoribbon

/Oligothiophene Composites. ACS Omega. 2022; 7(2):2260-2274.
2. Liu T, First EL, Hasan MMF, Floudas CA. Discovery of New Zeolites for H2S Removal through Multi-scale Systems Engineering, Comput. Aided Chem. Eng. 2015; 37:1025-1030. Doi: 10.1016/B978-0-444-63577-8.50016-4.
3. Sánchez M, Rincón M. Ammonia Sensors Based on Composites of Carbon Nanotubes and Titanium Dioxide, Carbon Nanotub. - Growth Appl, 2011. Doi: 10.5772/20466.
4. Lin SS. Light-emitting two-dimensional ultrathin silicon carbide, J. Phys. Chem. C. 2012; 116:3951-3955. Doi: https://doi.org/10.1021/JP210536M/SUPPL_FILE/JP210536M_SI_001.PDF.
5. Klinovaja J, Loss D. Spintronics in MoS_2 monolayer quantum wires, Phys. Rev. B - Condens. Matter Mater. Phys. 2013; 88(7). Doi: 10.1103/PhysRevB.88.075404.
6. Mortazavi B, Shahrokhi M, Raeisi M, Zhuang X, Pereira LFC, Rabczuk T. Outstanding strength, optical characteristics and thermal conductivity of graphene-like BC3 and BC6N semiconductors, Carbon N. Y. 2019; 149:733-742. Doi: https://doi.org/10.1016/J.CARBON.2019.04.084.
7. Vladimirov YA, Olenev VI, Suslova TB, Cheremisina ZP. Lipid peroxidation in mitochondrial membrane, Adv. Lipid Res. 1980; 17:173-249. Doi: 10.1016/b978-0-12-024917-6.50011-2.
8. Novoselov KS, *et al*. Two-dimensional gas of massless Dirac fermions in graphene, Nat. 2005; 438(7065):197-200. Doi: 10.1038/nature04233.
9. "No Title," [Online]. Available: Gaussian09, R. A. 1, mj frisch, gw trucks, hb schlegel, ge scuseria, ma robb, jr cheeseman, g. Scalmani, v. Barone, b. Mennucci, ga petersson *et al*., gaussian. Inc., Wallingford CT. 2009; 121:150-166.
10. Pacil̇ D, Meyer JC, Girit Ç, Zettl A. The two-dimensional phase of boron nitride: Few-atomic-layer sheets and suspended membranes, Appl. Phys. Lett. 2008; 92:133107. https://doi.org/10.1063/1.2903702.
11. Perdew JP, Burke K, Ernzerhof M. Generalized Gradient Approximation Made Simple. Phys. Rev. Lett. 1996; 77:3865-3868. Doi: https://doi.org/10.1103/physrevlett.77.3865.
12. Beheshtian J, Kamfiroozi M, Bagheri Z, Ahmadi A. Computational study of CO and NO adsorption on magnesium oxide nanotubes, Phys. E Low-Dimensional Syst. Nanostructures. 2011; 44(3):546-549. Doi: 10.1016/j.physe.2011.09.016.
13. Lin Y, Williams TV, Connell JW. Soluble, exfoliated hexagonal boron nitride nanosheets, J. Phys. Chem. Lett. 2010; 1:277-283. Doi: https://doi.org/10.1021/JZ9002108/SUPPL_FILE/JZ9002108_SI_001.PDF.
14. Aghaei SM, Monshi MM, Torres I, Calizo I. Adsorption and Dissociation of Toxic Gas Molecules on Graphene-like BC3: A Search for Highly Sensitive Molecular Sensors and Catalysts," Appl. Surf. Sci. 2017; 427:326-333. Doi: 10.1016/j.apsusc.2017.08.048.
15. Shlaka JA, Abo Nasria AH. Density functional theory study on the adsorption of AsH3 gas molecule with monolayer (AlN)21 (including pristine, C, B doped and defective aluminium nitride sheet)," IOP Conf. Ser. Mater. Sci. Eng. 2020; 928(7). Doi: 10.1088/1757-899X/928/7/072082
16. Lu N, Zhuo Z, Guo H, Wu P, Fa W, Wu X, Zeng XC. CaP3: A New Two-Dimensional Functional Material with Desirable Band Gap and Ultrahigh Carrier Mobility, J. Phys. Chem. Lett. 2018; 9:1728-1733. Doi: https://doi.org/10.1021/ACS.JPCLETT.8B00595.